JOURNAL OF MATERIALS SCIENCE 32 (1997) 4295–4301

Nanosecond pulsed excimer laser machining of chemical vapour deposited diamond and highly oriented pyrolytic graphite

Part I *An experimental investigation*

R. WINDHOLZ, P. A. MOLIAN
Mechanical Engineering Department, Iowa State University, Ames, IA 50011, USA

A laser beam offers the benefits of high precision, contamination-free, high speed, and low bulk temperature for machining of chemically vapour deposited (CVD) diamond thin films that in turn enable ultrafine finishing of diamond coated cutting tool inserts and drills, and for finishing and drilling of diamond coated multichip module applications. In this work, laser hole drilling and polishing of CVD diamond (free-standing diamond and coated tool inserts) and HOPG (highly oriented pyrolytic graphite) using a 248 nm wavelength, 23 ns pulsed excimer laser were conducted. The threshold energy fluence required for ablation of diamond and graphite was nearly the same but the material removal rate rapidly increases with the energy fluence for the graphite compared to diamond. At an energy fluence of 10 J cm^{-2}, the depth removed per pulse was 0.05 μm and 0.30 μm for diamond and graphite respectively. Raman microprobe analysis indicates that the laser machining induced the transformation of diamond to disordered forms of carbon in CVD diamond and some transformation of graphite to diamond in HOPG. The experimental data indicates that the transformation of diamond to graphite requires an energy input of 1.44×10^7 J per mole. For a given set of laser parameters, the depth per pulse was substantially higher for diamond coated tool inserts compared to the free-standing diamond. The surface roughness of CVD diamond was reduced by 0.25 μm per pulse at an energy fluence of 16 J cm^{-2}.

1. Introduction

Interest in diamond and diamond-like carbon (DLC) materials is driven by their extreme properties. Of all materials, diamond is harder than any known solid, has the highest elastic modulus, and has the highest thermal conductivity at room temperature. Diamond is chemically inert, and is highly transparent throughout a broad range of the optical spectrum. It is also a wide band gap semiconductor that is useful at high temperatures and high voltages. These properties, together with the ease of growth of diamond films by chemical vapour deposition (CVD), have made the material desirable for many applications such as heat spreaders, optical windows, X-ray lithography masks, low-friction and wear resistant surfaces, cutting tool coatings, and active electronic devices.

Diamond's hardness makes mechanical cutting, grinding, and polishing a time consuming and costly process. In the past, diamonds were commonly sawed using a thin wheel charged with diamond dust or cleaved with a tool along one of the crystallographic planes. This method was slow, failed in stones with faults in the path of the cut, and was limited to cuts along the "soft" cleavage planes. A laser, however, does not have any of the above restrictions. Drilling and cutting of natural diamond using infrared Nd:YAG lasers have been used for years as a means for rough shaping of industrial diamond and the removal of flaws from gems.

Gresser [1] performed some of the earliest work on laser machining of diamonds. He used a Q-switched Nd:YAG laser (1.06 μm wavelength) to cut gemstone diamonds, and cuts up to 3 mm deep and 0.5 mm wide were made. The laser beam was focused to a spot size of 0.025 mm, and the energy per pulse was 1.25×10^{-3} J, yielding an effective fluence of 247 J cm^{-2}. Using lasers also permitted Gresser to cut carbonado, a randomly oriented diamond crystal aggregate. The sawing of carbonado was previously impossible because a conventional diamond charged saw can not cut through certain planes of the carbonado.

The traditional method of polishing diamond is by grinding it on a flat wheel or scaife, typically about 300 mm in diameter, that is made from cast iron of carefully selected porosity. This scaife is charged with diamond powder ranging in sizes from less than 1 μm to 40 μm. Polishing is begun with coarse powder to give a faster removal rate, then finished with a finer powder to give a smooth surface finish. The surface to be polished is placed against the scaife, which is rotating near 2500 r.p.m. under a load of 1 kg. Today, the

0022–2461

cast iron scaife is often replaced by a wheel of similar geometry in which the diamond powder is bonded to a metal alloy or an organic resin on the surface of the wheel [2]. The resistance of diamond to polishing in this method greatly depends both on the crystallographic orientation of the face being polished and on the direction of polish on the face. Simply rotating the diamond through an angle of 45° can result in a reduction of the removal rate by a factor of 100. It is also necessary to avoid overheating the diamond due to the excessive load, as diamond can be readily burnt or damaged. A recent non-traditional method of etching crystalline diamond is ion-beam-assisted bombardment, where NO_2 molecules cause oxidation in the presence of a flux of Xe ions. In this method, the etch rate is about 200 nm per min [3]. However, this method is technologically disadvantageous due to its innate nature of introducing contaminants and roughness in the patterned regions [4].

CVD diamond films have received considerable attention in recent years because of their relative ease of growth and excellent properties. However, the growth of CVD diamond films results in faceted surfaces with a variation in peak-to-valley distance of 20–60 μm in 200 μm thick films. The rough surfaces of CVD diamond hinder their utility for optical coatings and cutting tools. For this reason, it is often desirable to finish-machine the diamond films. Most current CVD diamond finishing techniques have evolved from processes used for natural or synthetic diamonds.

Mechanical polishing or thinning of CVD diamond is time consuming and costly. Because of this, there have been other innovative attempts to polish CVD diamond films, such as the use of a reactive-ion oxygen beam [5, 6], contact with iron in a hydrogen atmosphere at elevated temperatures [7], or a combination of these two methods. The reactive-ion beam method is slow and is limited by the characteristics of the CVD film. The method involving the contact with iron at high temperatures is also limited because the high temperatures involved produce mechanical failure and thermal shocking of the film. Combining these two methods causes problems from the stresses and nonuniformities in the films themselves [8]. Edge Technology [9] polishes diamond films using a proprietary chemical polishing technique, and is able to achieve a roughness (arithmetic average) of 17 nm. This is considerably smoother than conventional polishing using diamond and carbide grit, which typically results in a roughness of 50 nm. Hashish and Bothell [8] have explored the use of abrasive liquid jets for polishing CVD diamond films, and they were able to polish a diamond film from 3 to 1.3 μm using SiC abrasives. Jin *et al.* [10] thinned and polished diamond films using a diffusional reaction at 1175 K with Mn and Fe metal powders and films. Using this process, they were able to reduce a free-standing diamond film from a thickness of 220 to 120 μm, and both the fine grained bottom region and most of the rough facets on the top surface were eliminated.

Although the methods described above have resulted in the removal of material from a diamond surface, none have demonstrated the combination of speed, resolution, and cost effectiveness needed to make them practical for widespread application [11]. Recently, it has been demonstrated that pulsed ultraviolet lasers offer a number of advantages for high-precision etching of diamond surfaces. These advantages include non-contact processing, contamination-free machining, precisely controlled removal rates, high energy delivered per pulse, and the ability to remove material from a minuscule area.

In this paper, we present an experimental study of 248-nm, KrF excimer laser machining of CVD diamond and HOPG (highly oriented pyrolytic graphite). The modelling and analysis of laser machined features will be presented in a companion publication.

2. Experimental procedure

2.1. Excimer laser and beam delivery system

Fig. 1 shows a sketch of the experimental setup used in this work. The excimer laser used was a Lambda-Physik Model LPX110i, the specifications of which are listed in Table 1. Both a constant energy mode and a constant voltage mode are available on this machine, but only the constant energy mode was used in these experiments.

A Laser Energetics Model LEX-BDS-1000992 beam delivery system [12] was used to deliver the laser beam to the workpiece. The system consists of five elements: a 200 mm telescope lens, a 100 mm telescope lens, a variable aperture, a turning mirror, and a 100 mm imaging lens. Fig. 2 shows the arrangement of these elements and the purpose of each item is discussed below.

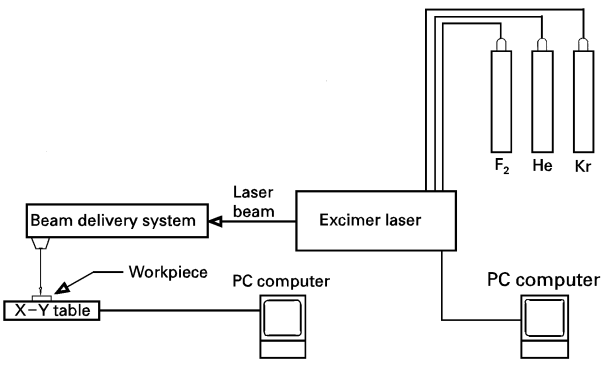

Figure 1 A schematic diagram of the experimental setup used in laser machining.

TABLE I Lambda physik LPX 110i laser specifications

Laser medium	KrF
Wavelength	248 nm
Maximum pulse rate	100 Hz
Maximum average power	30 W
Pulse width	23 ns
Beam dimensions	12 mm (Gaussian) × 23 mm (Flat-topped)
Beam divergence	1 × 3 mrad

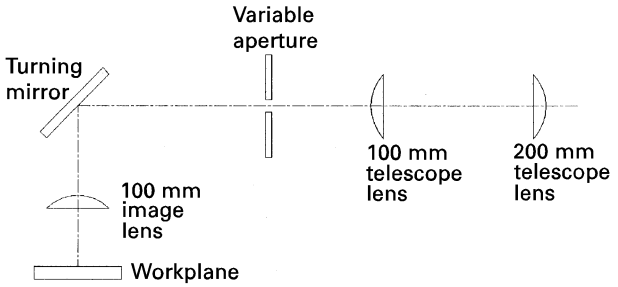

Figure 2 A schematic diagram of the beam delivery system.

2.1.1. Telescope lenses

The 200 and 100 mm telescope lenses are set in an confocal configuration, and increase the energy density on the aperture by a factor of four. An confocal configuration is one in which the focal points of two lenses are located at the same position. The laser beam is focused by the first lens at its focal point, and the focused laser beam then appears as a point light source which is imaged at infinity by the second lens.

2.1.2. Variable aperture

The variable aperture consists of two sets of knife blades which can be moved to change the spot size on the workpiece. The energy density on the workpiece is not affected by adjusting the aperture within the limit of the beam profile. However, the energy density and spot size can both change when the distance between the aperture and the imaging lens are changed.

2.1.3. Turning mirror

The turning mirror is used to redirect the laser beam to the workpiece. This mirror has a dielectric coating optimized for maximum reflection ($> 99.5\%$) at the 248 nm wavelength, so the optical losses are minimal.

2.1.4. Image lens

The image lens is used to project the aperture on the workpiece at a given demagnification ratio. The demagnification ratio, M, is defined as follows: $M = O/I$ where O is the object distance (the distance between the aperture and the image lens) and I is the image distance (the distance between the image lens and the workpiece). The following relation holds for O and I: $f^{-1} = O^{-1} + I^{-1}$ where f is the focal length of the image lens. Assuming no losses in the optics, the following relation holds for calculating E_{image}, the fluence at the image: $E_{\text{image}} = M^2 E_{\text{object}}$ where E_{object} is the fluence at the object. The image in this work was the workpiece, and the object was the variable aperture in the beam delivery system.

2.2. CVD diamond

Free-standing CVD diamond samples for this work were provided by the High Density Electronic Centre at the University of Arkansas. Films were grown on molybdenum substrates using a DC arc jet CVD process. A 1% methane in hydrogen at a flow rate 100 $\text{cm}^3\,\text{min}^{-1}$ was used as the precursor with typical deposition conditions of 1075–1175 K substrate temperature and 1.333×10^4 Pa pressure. Due to the mismatch in the coefficient of thermal expansion between the diamond and molybdenum, the diamond films "popped" off after deposition was completed. This typically resulted in free-standing diamond films with dimensions $10 \times 10 \times 0.5$ mm thick. The impurities in the samples were graphite and hydrogen. CVD diamond typically also has crystal defects such as some amorphous structure, twinning on (1 1 1) planes due to stacking faults, and many grain boundaries. Unfortunately, a standardized classification scheme for CVD diamond does not exist unlike the natural or synthetic diamond types.

The substrate side of the free-standing diamond films was relatively smooth, but the deposition side was rough, with average values of surface roughness around 7–8 μm in arithmetic average scale. This roughness was due to the polycrystalline growth of the diamond crystals. The crystals on the rough side of the free-standing diamond samples have an orientation that depended on growth conditions. The (1 1 1) and (1 1 0) orientations were predominant in the provided films. These samples with the rough deposition side were used in this work to study the effect of laser fluence on surface roughness. Some of the free-standing diamond samples were polished using mechanical lapping at the University of Arkansas before they were sent to us for laser processing. These samples provided easier measurement of ablated hole depths.

2.3. Highly oriented pyrolytic graphite

One special form of graphite, pyrolytic graphite, is produced using a CVD process similar to that used for CVD diamond production. Highly oriented pyrolytic graphite (HOPG) is the most orderly form of this product. The nature and properties of HOPG closely match that of ideal graphite crystals. Because of this, it can be assumed that HOPG provides a good representation of the graphite likely to be formed on the diamond surface by a laser. The HOPG used in this work had dimensions of $12 \times 12 \times 2$ mm, and was a grade ZYB pyrolytic graphite monochromator purchased from Advanced Ceramics Corporation, Cleveland, OH.

2.4. Experimental procedure

Two types of laser machining, hole drilling and polishing, were conducted. The pulse energy was varied between 9–300 mJ, and the imaging optics were adjusted to allow a range of fluences between 0.94–38.4 $\text{J}\,\text{cm}^{-2}$. A series of blind holes was produced using 100 pulses at a pulse repetition rate of 1 Hz. A few experiments were also performed as a function of pulse repetition rate up to 8 Hz. A Dektak profilometer (resolution 300 nm) was then used to obtain hole profiles and measure the hole depth. Scanning electron microscopy (SEM) was used to examine the

TABLE II Raman spectrometer conditions and data

Sample	ID	Power/slit	Scan (cm^{-1})
CVD diamond	Untreated PMCD02	100 mW/ 100 μm	1300–1360
CVD diamond	Laser treated PMCD05	100 mW/ 200 μm	1300–1360
HOPG	Untreated PMHG05	200 mW/ 600 μm	1000–1800
HOPG	Laser treated PMHG06	200 mW/ 600 μm	1000–1800

hole characteristics. In laser polishing, the sample was moved on an XY table while the laser beam was stationary. The speed of the table was adjusted to allow an exposure of 10 or 20 pulses in each area, and successive laser spots were superimposed. A Dektak profilometer was then used to measure the surface roughness before and after polishing.

2.5. Raman spectroscopy

Raman microprobe analysis of laser machined CVD diamond and HOPG was carried out to identify the transformation of diamond to graphite or *vice-versa*. Raman experiments were performed at the Material Research Lab in Pennsylvania State University using an ISA U-1000 Raman spectrometer in the micromode (with a 40X objective) and using an Ar-ion laser under the conditions shown in Table II.

3. Results and discussion

Fig. 3 (a and b) shows SEM micrographs of the holes produced in CVD diamond and HOPG samples. The large white particles in and around the hole in the CVD diamond sample are miscellaneous debris that was not present immediately after ablation occurred. Looking closely at the holes, there appears to be many ridges radiating from the centre of the hole. In some places, these ridges appear roughly periodic. They follow a pattern that suggests that the ridges are caused by consistent variations in the beam energy distribution. The output of excimer lasers is inherently multimode, so the ridges may be created by many small "near-Gaussian" beams next to each other in the excimer laser beam. Although the roughness of the laser etched surface resembled the mode print, the difference in the etch rates between diamond and graphite suggests that it is also due to photoetching. In HOPG, the debris near the perimeter of the hole (Fig. 3b) appears to have been blown away. The debris consists of several distinct layers of graphite, and may have been produced by an elastic wave generated by transient surface heating [13] or a high pressure shock wave associated with plume formation [14, 15]. A high pressure shock wave could easily remove layers of material near the hole perimeter since there are probably minuscule gaps between the graphite sheets, and the bonding strength between sheets is very weak.

Ageev *et al.* [16] observed linear periodic structures on the surface of diamond films that had been irradiated with a CO_2 laser. The period of the structures

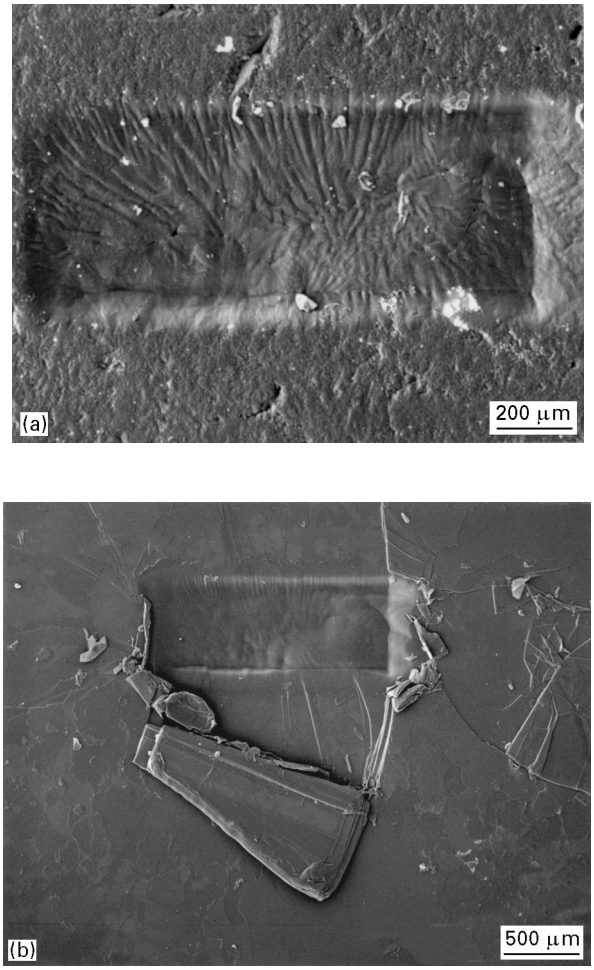

Figure 3 Scanning electron microscopy (SEM) micrographs of laser-cut holes (a) CVD diamond (b) HOPG.

was about 10 μm, which is close to the wavelength of CO_2 lasers (10.6 μm). Ageev *et al.* postulated that these structures appeared as a result of the interference of the incident and scattered light waves. This interference caused a spatial modulation of the absorbed intensity, resulting in a spatial modulation of the surface temperature of the diamond. The periodic profile of the distribution of the temperature and thermal stresses in the laser spot then led to the formation of a relief as a result of the evaporation and removal of material. The periodicity of the structures in Fig. 3 (a and b) appears to be much larger than the wavelength of a KrF laser (248 nm), so a mechanism different from that observed by Ageev *et al.* might have occurred.

As opposed to the CVD diamond holes, the edges of all HOPG holes are sharp, which is the normal behaviour for most materials cut with excimer lasers. The difficulty in obtaining sharp edges with diamond is attributed to the low energy spots at the edges of the beam. These low energy areas then produced a hole pattern that was similar to the energy distribution across the aperture. The rounded edges may also be due to a buildup of vapour pressure in the blind hole, which could have expelled some material.

Surface profilometer readings of the holes cut in CVD diamond and HOPG are shown in Fig. 4 (a and b). The uneven bottom of the hole, typical of all the holes made in this work, was probably caused by the

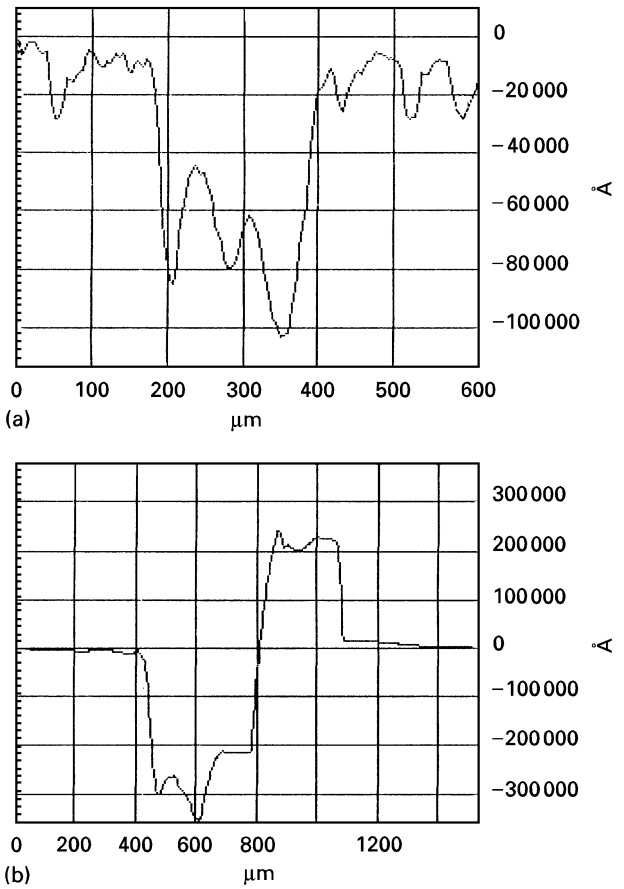

Figure 4 Profilometer scans of holes cut in (a) CVD diamond (b) HOPG.

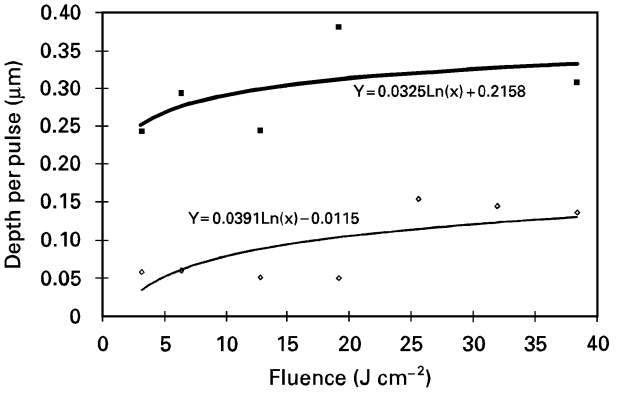

Figure 5 Variation of etch depth per pulse with energy fluence for (◇) diamond and (■) HOPG. The curves represent (—) Log. (diamond) and (▬) Log. (HOPG).

non-symmetric nature of the beam distribution. Plume absorption of energy may also have contributed to this unevenness. The hole profile may also be a result of the combined effect of attenuation of the centre portion of the beam by the ablated material and redeposition of the ablated material as proposed by Inam *et al.* [17] and observed by Prawer *et al.* [18].

Fig. 5 shows the data obtained relating fluence and ablation rate for both CVD diamond and HOPG ablated under similar conditions. Using a "best fit" logarithmic line and extrapolating it to the x-axis, the threshold fluence for ablation was estimated to be $0.8\ J\,cm^{-2}$ for CVD diamond. Due to equipment limitations, this threshold fluence could not be accurately verified in the laboratory. The lowest experimental fluence that could be generated was $0.94\ J\,cm^{-2}$ and this fluence appears to be close to the threshold fluence for HOPG. For fluences above the threshold and below $3.2\ J\,cm^{-2}$, the etch rate for HOPG rises rapidly as a function of fluence. This means that if a well stabilized laser with an accurately measurable output is used for etching, the desirable region where etching can be performed most efficiently is approximately between 1–$3.2\ J\,cm^{-2}$. However, if the laser output is not easily definable or stable, then etching in the region where the fluence is higher than $3.2\ J\,cm^{-2}$ may be more suitable. In the region above $3.2\ J\,cm^{-2}$, the etch rate is not very sensitive to small variations in fluence, so a steady etch rate can be easily maintained.

From the similarity of the etch rate curves obtained for free-standing CVD diamond and HOPG shown in Fig. 5, the ablation behaviour of HOPG is similar to that of diamond and they differ mainly in their vertical distance from each other. This distance is 0.227 μm per pulse, and represents the energy required to convert diamond to graphite. Using this distance, one can calculate that it takes approximately 1.44×10^7 J per mole to convert diamond to graphite. Fig. 5 also shows that the amount of diamond being converted to graphite dramatically grows as the fluence increases until it reaches a value around $3.2\ J\,cm^{-2}$. After that, further increases in energy do not significantly increase the volume converted to graphite. This may be due to a combination of energy absorption by the plume and attainment of the maximum thermal penetration depth.

Figs. 6 (a and b) and 7 (a and b) show the representative Raman spectra of untreated and laser machined CVD diamond and graphite samples. In the laser machined CVD diamond, several forms of disordered carbon were observed. Some regions were amorphous carbon (1343 and 1591 cm^{-1}) while other regions were diamond (1332 cm^{-1}) and polycrystalline graphite (1580 cm^{-1}). In the case of laser machined graphite, it is interesting to note that there is evidence for diamond suggesting that the laser beam provides sufficient energy to enable the transformation of graphite to diamond.

Fig. 8 shows the variation of etch depth per pulse in free-standing CVD diamond as a function of pulse repetition rate at a constant pulse energy. The etch depth per pulse decreases in a near linear manner as the pulse repetition rate increases. Although no adequate explanation for this effect can be offered, a possible explanation may be the energy absorption by the plasma plume, which exists for a short time after the end of each laser pulse. As the pulse repetition rate is increased, some of the laser energy might be absorbed by the plume from the previous pulse. Absorption of energy by the plume has also been proposed by Tonshoff and von Alvensleben [19].

Along with ablating free-standing CVD diamond samples, experiments were also conducted on a CVD diamond coated carbide tool. The coating with

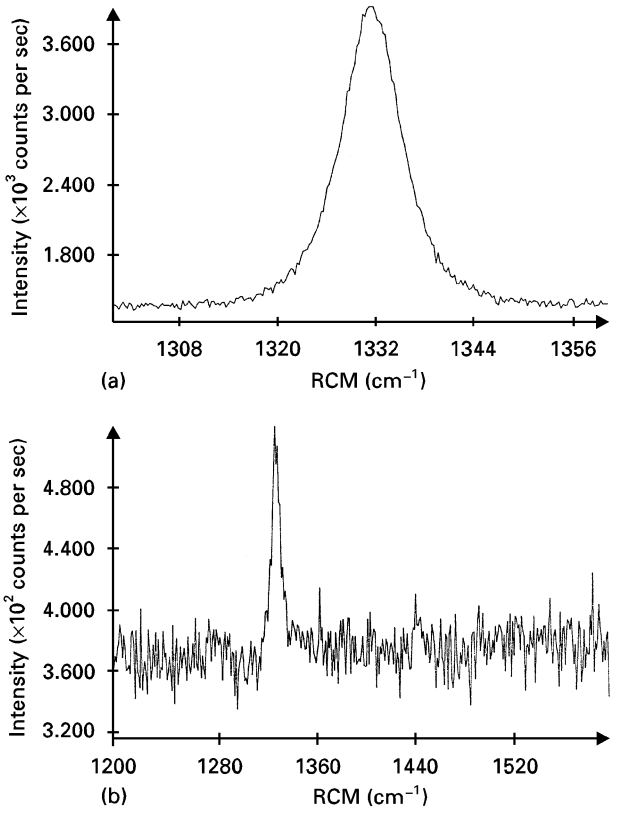

Figure 6 Raman spectra of CVD diamond in the (a) as-received condition (b) laser machined condition.

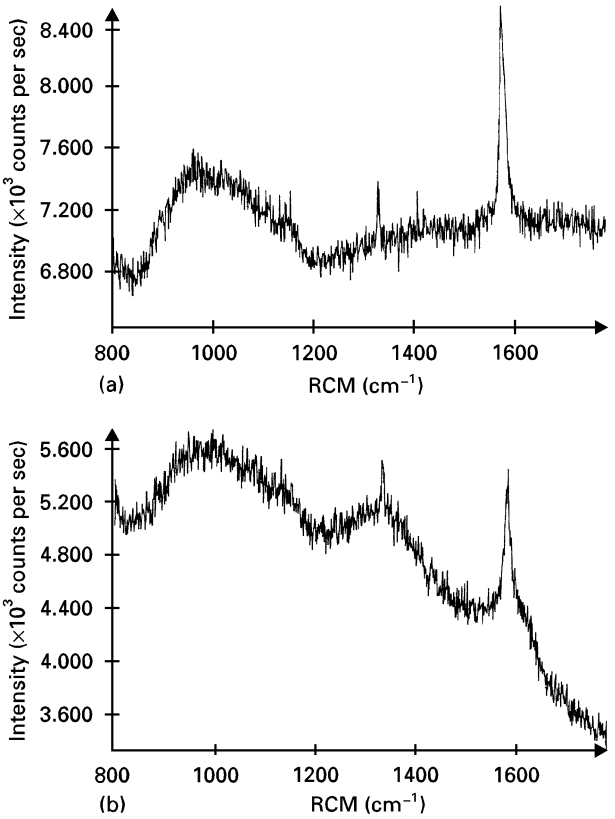

Figure 7 Raman spectra of HOPG in the (a) as-received condition (b) laser machined condition.

a thickness of 14 μm was removed in three laser pulses at 5.6 J cm^{-2} (Fig. 9). This yields an overall etch rate of 4.6 μm per pulse, which is considerably higher than the value obtained for the free-standing CVD

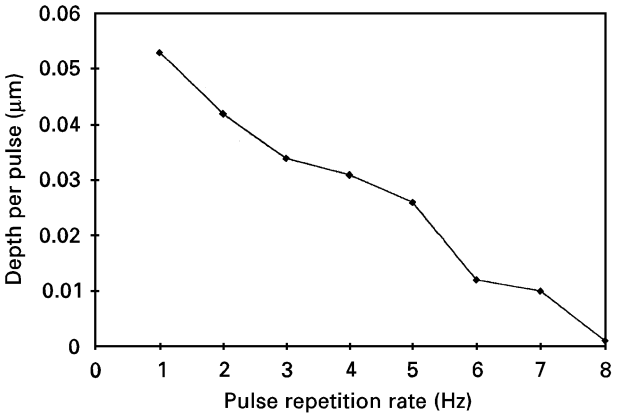

Figure 8 Variation of etch depth per pulse with pulse repetition rate for CVD diamond.

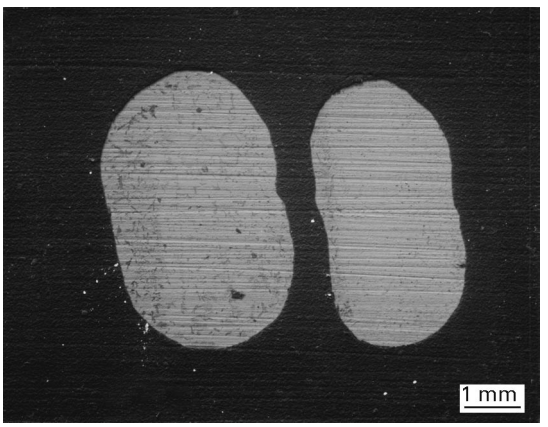

Figure 9 SEM micrograph of typical holes cut in diamond coated carbide tool.

diamond, and this is probably due to the different properties of the coating. In support of this, Kononenko *et al.* [20] noted that the etch rate was higher for less dense diamond like carbon films because they have a higher absorption coefficient. Fig. 10 shows a profilometer measurement of the CVD coated tool after exposure to a single pulse at 5.6 J cm^{-2}. A "hill" was formed which appeared dark in colour, indicating that the surface of the diamond had been transformed into graphite. The density of graphite is lower than that of diamond, so when diamond changes into graphite, it expands and takes up a larger volume. This explains the appearance of the "hill" on the surface of the CVD diamond film.

Laser polishing experiments to reduce the surface roughness were conducted using a fluence of 16 J cm^{-2} and a pulse repetition rate of 5 Hz. The surface roughness was reduced at a rate of 0.25 μm per pulse. Fig. 11 shows two polished lines that were produced by scanning the laser beam across the surface. A closer examination revealed that the peaks of the diamond crystals have been mostly removed. Kononenko *et al.* [20] was able to reduce the surface roughness by an order of magnitude in laser polished diamond. He also experimentally determined that the surface roughness depended on the angle of laser beam incidence. Tokarev and Konov [21] developed a complex model for the laser polishing of diamond film.

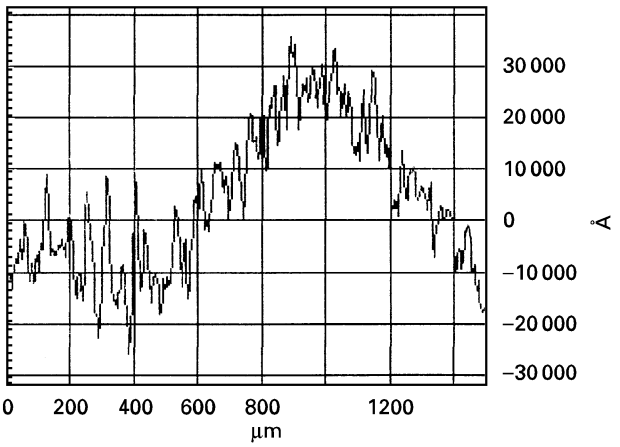

Figure 10 Profilometer scan of the graphite "hill" in the CVD diamond coated tool insert.

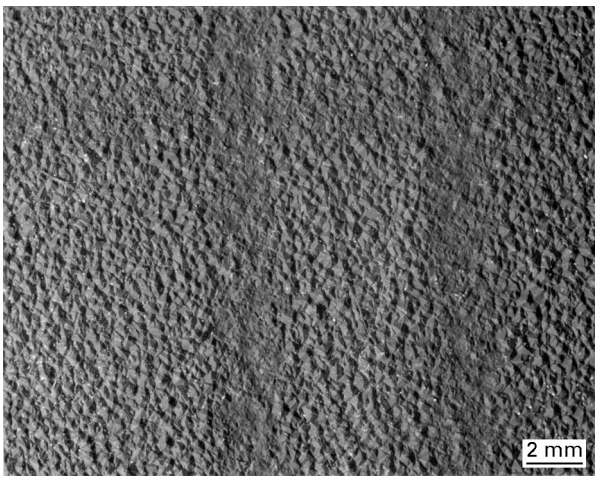

Figure 11 SEM micrograph of the two lines scanned on the rough side of free-standing CVD diamond.

4. Conclusions

A 23 ns pulsed KrF excimer laser was employed to investigate the machining behaviour of CVD diamond and HOPG. The relationship between etch depth per pulse and fluence was determined, along with the minimum fluence required for etching to occur. The etch depth per pulse for both CVD diamond and HOPG followed a logarithmic relationship typical of laser ablation for many materials. The data allowed a calculation of the energy needed to convert diamond to graphite, which was determined to be approximately 1.44×10^7 J per mole. Raman microprobe spectroscopy analysis revealed that there is a transformation of diamond to disordered forms of carbon during laser machining of CVD diamond, and there is some transformation of graphite to diamond during laser machining of HOPG. Limited experiments, conducted using the nanosecond KrF laser to reduce the surface roughness of as-grown CVD diamond film, showed that the surface roughness could be substantially reduced. This demonstrates the potential for using lasers to smoothen the rough surfaces of CVD diamond.

Acknowledgements

The authors would like to acknowledge the financial support provided by the National Science Foundation under the contract DMI 9504102. Thanks should also go to Dr Ajay Malshe for providing the CVD diamond samples used in this work.

References

1. H. D. GRESSER, Laser sawing of diamonds, Dearborn, MI, 1976. Technical Paper MR76-855 (Society of Manufacturing Engineers, Dearborn, MI, 1976) pp. 1–11.
2. J. WILKS and E. WILKES, "Properties and Applications of Diamond" (Courier International Ltd., Boston, MA, 1991).
3. M. ROTHSCHILD, C. ARNONE and D. J. EHRLICH, *J. Vac. Sci. Technol. B* **4** (1986) 310.
4. A. P. MALSHE, S. T. KSHIRSAGAR and K. S. CHARI, *Mater. Lett.* **11** (1991) 175.
5. A. HIRATA, H. TOKURA and M. YOSHIKAWA, in "Applications of Diamond Films and Related Materials", edited by Y. Tzeng (Elsevier, New York, 1991) pp. 227–232.
6. N. N. EFREMOW, M. W. GEIS, D. C. FLANDERS, G. A. LINCOLN and N. P. ECONOMOU, *J. Vac. Sci. Technol. B* **3** (1985) 416.
7. A. B. HARKER, in "Applications of Diamond Films and Related Materials", edited by Y. Tzeng (Elsevier, New York, 1991) pp. 223–225.
8. M. HASHISH and D. H. BOTHELL, in "Diamond Optics V", SPIE Vol. 1759, edited by A. Feldman and S. Holly (The Society of Photo-Optimal Instrumentation Engineers, Bellingham, WA, 1992) pp. 97–105.
9. M. B. MORAN, K. A. KLEMM and L. F. JOHNSON, in "Applications of Diamond Films and Related Materials", edited by Y. Tzeng (Elsevier, New York, 1991) p. 236.
10. S. JIN, J. E. GRAEBNER and T. H. TIEFEL, in "Diamond Optics V", SPIE Vol. 1759, edited by A. Feldman and S. Holly (The Society of Photo-Optimal Instrumentation Engineers, Bellingham, WA, 1992) pp. 57–67.
11. C. P. CHRISTENSEN, in "Lasers as Tools for Manufacturing", SPIE Vol. 2062, edited by L. Migliore and R. Walker (The Society of Photo-Optimal Instrumentation Engineers, Bellingham, WA, 1993) pp. 14–21.
12. Laser Energetics Inc. LEX-BDS-1000992 Beam Delivery System Laser Energetics Inc, Orlando, FL.
13. R. M. WHITE, *J. Appl. Phys.* **34** (1963) 3559.
14. R. BULLOUGH and J. J. GILMAN, *ibid.* **37** (1966) 2283.
15. D. BAUERLE, In "NATO ASI series E: applied sciences Vol. 265", Excimer Lasers, edited by L. Laude (Kluwer Academic Publishers, Boston, MA, 1994) p. 44.
16. V. P. AGEEV, L. L. BUILOV, V. I. KONOV, A. V. KUZMICHEV, S. M. PIMENOV and A. M. PROKHOROV, *Dokl. Akad. Nauk SSSR* **303** (1988) 598.
17. A. INAM, X. D. WU, T. VENKATESAN, S. B. OGALE, C. C. CHANG and D. DIJKKAMP, *Appl. Phys. Lett.* **51** (1987) 1112.
18. S. PRAWER, R. KALISH and M. ADEL, *ibid.* **48** (1986) 1585.
19. H. K. TONSHOFF and F. VON ALVENSLEBEN, in "Solid State Lasers IV", SPIE Vol. 1864, edited by G. Quarles and M. Woodhill (The Society of Photo-Optimal Instrumentation Engineers, Bellingham, WA, 1993) pp. 96–107.
20. T. V. KONONENKO, V. I. KONOV and V. G. RALCHENKO, in "Diamond Optics V", SPIE Vol. 1759, edited by A. Feldman and S. Holly (The Society of Photo-Optical Instrumentation Engineers, Bellingham, WA, 1992) pp. 106–114.
21. V. N. TOKAREV and V. I. KONOV, in "Applications of Diamond Films and Related Materials", edited by Y. Tzeng (Elsevier, New York, 1991) pp. 249–255.

Received 19 April
and accepted 30 October 1996